第 35 卷第 7 期
2019 年 7 月

无 机 化 学 学 报
CHINESE JOURNAL OF INORGANIC CHEMISTRY

Vol.35 No.7
1248-1254

两个包含联苯类三羧酸配体的钴(Ⅱ)和镍(Ⅱ)配位聚合物的合成、晶体结构及磁性质

赵 娜 黎 彧* 冯安生 邹训重*

(广东轻工职业技术学院,广东省特种建筑材料及其绿色制备工程技术研究中心/
佛山市特种功能性建筑材料及其绿色制备技术工程中心,广州 510300)

摘要:采用水热方法,用 2 种联苯类三羧酸配体:联苯-2,4,4′-三羧酸(H_3btc)、5-(3,4-二羧基苯基)吡啶甲酸(H_3dppa)和 4,4′-联吡啶(4,4′-bipy)分别与 $CoCl_2·6H_2O$ 和 $NiCl_2·6H_2O$ 反应,合成了具有一维双螺旋链结构的配合物$[Co(\mu_2\text{-}H_2btc)_2(4,4'\text{-bipy})_2]_n$ (**1**)以及二维层状配位聚合物$\{[Ni_3(\mu_4\text{-dppa})_2(H_2O)_6]·2H_2O\}_n$ (**2**),并对其结构和磁性质进行了研究。结构分析结果表明 2 个配合物都属于三斜晶系,$P\bar{1}$ 空间群。配合物 **1** 具有一维双螺旋链结构,而且这些链通过 O–H···O/N 氢键作用进一步形成了三维超分子框架。而配合物 **2** 具有基于一维链单元的二维层状结构。4,4′-联吡啶在配合物 **1** 和 **2** 中分别起配位作用和模板作用。研究表明,配合物 **1** 中相邻钴离子间存在铁磁相互作用。

关键词:配位聚合物;双螺旋链;模板效应;三羧酸配体;磁性
中图分类号:O614.81+2;O614.81+3 **文献标识码**:A **文章编号**:1001-4861(2019)07-1248-07
DOI:10.11862/CJIC.2019.094

Syntheses, Crystal Structures, and Magnetic Properties of Two Cobalt(Ⅱ) and Nickel(Ⅱ) Coordination Polymers Constructed from Biphenyl-Type Tricarboxylic Acids

ZHAO Na LI Yu* FENG An-Sheng ZOU Xun-Zhong*

(*Guangdong Research Center for Special Building Materials and Its Green Preparation Technology/ Foshan Research Center for Special Functional Building Materials and Its Green Preparation Technology, Guangdong Industry Polytechnic, Guangzhou* 510300, *China*)

Abstract: Two 1D cobalt(Ⅱ) and 2D nickel(Ⅱ) coordination polymers, namely $[Co(\mu_2\text{-}H_2btc)_2(4,4'\text{-bipy})_2]_n$ (**1**) and $\{[Ni_3(\mu_4\text{-dppa})_2(H_2O)_6]·2H_2O\}_n$ (**2**), have been constructed hydrothermally using H_3btc (H_3btc=biphenyl-2,4,4′-tricarboxylic acid), H_3dppa (H_3dppa =5-(3,4-dicarboxylphenyl)picolinic acid), 4,4′-bipy(4,4′-bipy=4,4′-bipyridine), and cobalt or nickel chlorides. Single-crystal X-ray diffraction analyses reveal that both compounds crystallize in the triclinic system, space group $P\bar{1}$. Compound **1** has a 1D double-helix chain structure, which is assembled to a 3D supramolecular framework through O–H···O/N hydrogen bond. Compound **2** shows a 2D sheet based on 1D chain units. Moreover, 4,4′-bipy can tune the structures of both coordination polymers by its coordination or template effect. Magnetic studies for compound **1** demonstrate a ferromagnetic coupling between the adjacent Co(Ⅱ) centers. CCDC: 1889686, **1**; 1889687, **2**.

Keywords: coordination polymer; double-helix chain; template effect; tricarboxylic acid; magnetic properties

收稿日期:2019-01-10。收修改稿日期:2019-03-01。
广东省高等职业院校珠江学者岗位计划资助项目(2015,2018),广东省自然科学基金(No.2016A030313761),广东轻院珠江学者人才类项目(No.RC2015-001),生物无机与合成化学教育部重点实验室开放基金(2016),广东省高校创新团队项目(No.2017GKCXTD001),广州市科技计划项目(No.201904010381)和广东省高校特色创新项目(No.2017GKTSCX005)资助。
*通信联系人。E-mail:liyuletter@163.com,2017018009@gdip.edu.cn

0 Introduction

Coordination polymers have attracted tremendous attention owing to their intriguing architectures and topologies, as well as potential applications in catalysis, magnetism, luminescence, molecular sensing, and gas absorption[1-8]. However, it is difficult to predict the structure of a coordination polymer, because there are many factors, such as the coordination geometry of the metal centers, type and connectivity of organic ligands, stoichiometry, reaction conditions, template effect, presence of auxiliary ligands, and pH values influencing the structures of target coordination polymers during self-assembly[9-14]. Undoubtedly, organic ligands play a crucial role in the construction of coordination polymers.

As we known, the multi-carboxylate biphenyl-type ligands have been certified to be of great significance as constructors due to their abundant coordination modes, which could satisfy different geometric requirements of metal centers[13-20]. Besides the main organic building blocks, many other components of a reaction system such as co-ligands or template agents can also play an important role in the generation of coordination polymers[21-22]. It is well known that co-ligands coordinate to metal centers as ancillary moieties, while the template agents do not coordinate to metal centers and often do not enter into the final structure, but have a structure-guiding behavior during the self-assembly synthesis. 4,4′-Bipyridine (4,4′-bipy) represents one of the most common examples of such a co-ligand or template agent[14,23-24].

Therefore, based on the above reasons, we designed and synthesized two Co(Ⅱ) and Ni(Ⅱ) coordination polymers based on two biphenyl-type tricarboxylate ligands: biphenyl-2,4,4′-tricarboxylic acid (H_3btc) and 5-(3,4-dicarboxylphenyl)picolinic acid (H_3dppa). In this article, we report the syntheses, crystal structures, and magnetic properties of two Co(Ⅱ) and Ni(Ⅱ) coordination polymers constructed from biphenyl-type tricarboxylate ligands.

1 Experimental

1.1 Reagents and physical measurements

All chemicals and solvents were of AR grade and used without further purification. Carbon, hydrogen and nitrogen were determined using an Elementar Vario EL elemental analyzer. IR spectra were recorded using KBr pellets and a Bruker EQUINOX 55 spectrometer. Thermogravimetric analysis (TGA) data were collected on a LINSEIS STA PT1600 thermal analyzer with a heating rate of 10 ℃·min^{-1}. Magnetic susceptibility data were collected in the 2~300 K temperature range on a Quantum Design SQUID Magnetometer MPMS XL-7 with a field of 0.1 T. A correction was made for the diamagnetic contribution prior to data analysis.

1.2 Synthesis of $[Co(\mu_2\text{-}H_2btc)_2(4,4'\text{-bipy})_2]_n$ (1)

A mixture of $CoCl_2 6H_2O$ (0.036 g, 0.15 mmol), H_3btc (0.086 g, 0.30 mmol), 4,4′-bipy (0.047 g, 0.3 mmol), NaOH (0.012 g, 0.30 mmol), and H_2O (10 mL) was stirred at room temperature for 15 min, and then sealed in a 25 mL Teflon-lined stainless steel vessel, and heated at 160 ℃ for 3 days, followed by cooling to room temperature at a rate of 10 ℃·h^{-1}. Pink block-shaped crystals of **1** were isolated manually, and washed with distilled water. Yield: 55% (based on H_3btc). Anal. Calcd. for $C_{50}H_{34}CoN_4O_{12}$(%): C 63.77, H 3.64, N 5.95; Found(%): C 63.44, H 3.61, N 5.98. IR (KBr, cm^{-1}): 1 677s, 1 604s, 1 571s, 1 414m, 1 375w, 1 319w, 1 287s, 1 237w, 1 209w, 1 174w, 1 119w, 1 097w, 1 069w, 1 008w, 914w, 840w, 812m, 763m, 706w, 685w, 622w.

1.3 Synthesis of $\{[Ni_3(\mu_4\text{-dppa})_2(H_2O)_6]\cdot 2H_2O\}_n$ (2)

A mixture of $NiCl_2\cdot 6H_2O$ (71.0 mg, 0.30 mmol), H_3dppa (57.4 mg, 0.20 mmol), 4,4′-bipy (0.047 g, 0.3 mmol), NaOH (24.0 mg, 0.60 mmol), and H_2O (10 mL) was stirred at room temperature for 15 min, then sealed in a 25 mL Teflon-lined stainless steel vessel, and heated at 160 ℃ for 3 days, followed by cooling to room temperature at a rate of 10 ℃·h^{-1}. Green block-shaped crystals of **2** were isolated manually, washed with distilled water, and dried. Yield: 60%

(based on H_3dppa). Anal. Calcd. for $C_{28}H_{28}Ni_3N_2O_{20}$(%): C 37.84, H 3.18, N 3.15; Found(%): C 38.06, H 3.19, N 3.17. IR (KBr, cm^{-1}): 3 440m, 3 067w, 1 627m, 1 597s, 1 495w, 1 474w, 1 444m, 1 368m, 1 311w, 1 240w, 1 158 w, 1 117w, 1 087w, 1 041w, 1 016w, 852w, 817w, 776m, 735w, 709w, 654w.

The compounds are insoluble in water and common organic solvents, such as methanol, ethanol, acetone and DMF.

1.4 Structure determinations

Two single crystals with dimensions of 0.27 mm×0.22 mm×0.21 mm (**1**) and 0.25 mm×0.23 mm×0.21 mm (**2**) were collected at 293(2) K on a Bruker SMART APEX Ⅱ CCD diffractometer with Mo $K\alpha$ radiation (λ=0.071 073 nm). The structures were solved by direct methods and refined by full matrix least-square on F^2 using the SHELXTL-2014 program[25]. All non-hydrogen atoms were refined anisotropically. All the hydrogen atoms except those of the water molecules in **2** were positioned geometrically and refined using a riding model. The hydrogen atoms of the water molecules in **2** were located from the difference Fourier maps. A summary of the crystallography data and structure refinements for **1** and **2** is given in Table 1. The selected bond lengths and angles for compounds **1** and **2** are listed in Table 2. Hydrogen bond parameters of compounds **1** and **2** are given in Tables 3 and 4.

CCDC: 1889686, **1**; 1889687, **2**.

Table 1 Crystal data for compounds 1 and 2

Compound	**1**	**2**
Chemical formula	$C_{50}H_{34}CoN_4O_{12}$	$C_{28}H_{28}Ni_3N_2O_{20}$
Molecular weight	941.74	888.65
Crystal system	Triclinic	Triclinic
Space group	$P\bar{1}$	$P\bar{1}$
a / nm	0.971 35(3)	0.750 36(9)
b / nm	1.376 38(6)	0.958 82(12)
c / nm	1.643 05(8)	1.202 12(15)
α / (°)	72.953(4)	88.205(10)
β / (°)	80.308(4)	75.631(11)
γ / (°)	77.675(3)	76.874(10)
V / nm^3	2.038 55(16)	0.815 64(18)
Z	2	1
F(000)	970	454
θ range for data collection / (°)	3.235~25.049	3.309~25.043
Limiting indices	$-11 \leqslant h \leqslant 11, -15 \leqslant k \leqslant 16, -19 \leqslant l \leqslant 17$	$-8 \leqslant h \leqslant 8, -10 \leqslant k \leqslant 11, -14 \leqslant l \leqslant 10$
Reflection collected, unique (R_{int})	11 987, 7 234 (0.023 5)	2 883, 5 852 (0.061 3)
D_c / ($g\cdot cm^{-3}$)	1.534	1.809
μ / mm^{-1}	0.498	1.807
Data, restraint, parameter	7 234, 0, 606	2 883, 0, 241
Goodness-of-fit on F^2	0.998	1.030
Final R indices [$I \geqslant 2\sigma(I)$] R_1, wR_2	0.043 6, 0.105 4	0.064 8, 0.130 3
R indices (all data) R_1, wR_2	0.054 7, 0.114 1	0.104 5, 0.161 2
Largest diff. peak and hole / ($e\cdot nm^{-3}$)	383 and −359	744 and −653

Table 2 Selected bond distances (nm) and bond angles (°) for compounds 1 and 2

1					
Co(1)-O(1)	0.210 9(2)	Co(1)-O(2)A	0.204 6(2)	Co(1)-O(7)	0.210 6(2)
Co(1)-O(8)B	0.204 3(2)	Co(1)-N(1)	0.217 8(2)	Co(1)-N(3)	0.216 5(2)

Continued Table 2

O(8)B-Co(1)-O(2)A	174.50(7)	O(8)B-Co(1)-O(7)	91.25(7)	O(2)A-Co(1)-O(7)	88.89(7)
O(8)B-Co(1)-O(1)	88.75(7)	O(2)A-Co(1)-O(1)	90.25(7)	O(7)-Co(1)-O(1)	170.95(7)
O(8)B-Co(1)-N(3)	91.77(7)	O(2)A-Co(1)-N(3)	93.69(7)	O(7)-Co(1)-N(3)	94.68(7)
O(1)-Co(1)-N(3)	94.37(7)	O(8)B-Co(1)-N(1)	87.87(7)	O(2)A-Co(1)-N(1)	86.66(7)
O(7)-Co(1)-N(1)	85.62(7)	O(1)-Co(1)-N(1)	85.34(7)	N(3)-Co(1)-N(1)	179.55(8)
		2			
Ni(1)-O(2)	0.205 1(4)	Ni(1)-O(3)A	0.212 1(5)	Ni(1)-O(6)A	0.203 8(5)
Ni(1)-O(7)	0.208 2(5)	Ni(1)-O(8)	0.209 0(5)	Ni(1)-N(1)	0.212 0(5)
Ni(2)-O(5)	0.206 7(4)	Ni(2)-O(5)B	0.206 7(4)	Ni(2)-O(4)C	0.214 8(4)
Ni(2)-O(4)D	0.214 8(4)	Ni(2)-O(9)	0.211 7(5)	Ni(2)-O(9)B	0.211 7(5)
O(6)A-Ni(1)-O(2)	173.2(2)	O(6)A-Ni(1)-O(7)	90.1(2)	O(2)-Ni(1)-O(7)	91.14(19)
O(6)A-Ni(1)-O(8)	87.8(2)	O(2)-Ni(1)-O(8)	99.0(2)	O(7)-Ni(1)-O(8)	85.3(2)
O(6)A-Ni(1)-N(1)	99.6(2)	O(2)-Ni(1)-N(1)	78.71(18)	O(7)-Ni(1)-N(1)	169.2(2)
O(8)-Ni(1)-N(1)	99.9(2)	O(6)A-Ni(1)-O(3)A	87.7(2)	O(3)A-Ni(1)-O(2)	85.8(2)
O(7)-Ni(1)-O(3)A	87.2(2)	O(8)-Ni(1)-O(3)A	171.1(2)	N(1)-Ni(1)-O(3)A	88.4(2)
O(5)B-Ni(2)-O(9)B	94.6(2)	O(5)-Ni(2)-O(9)B	85.4(2)	O(5)B-Ni(2)-O(4)D	91.4(2)
O(5)-Ni(2)-O(4)D	88.6(2)	O(9)B-Ni(2)-O(4)D	86.3(2)	O(9)-Ni(2)-O(4)D	93.7(2)

Symmetry codes: A: $-x$, $-y+2$, $-z+2$; B: $-x+1$, $-y+2$, $-z+2$ for **1**; A: $-x+2$, $-y+2$, $-z+2$; B: $-x+1$, $-y+2$, $-z+3$; C: $x-1$, y, z; D: $-x+2$, $-y+3$, $-z+3$ for **2**.

Table 3　Hydrogen bond parameters of compound 1

D–H…A	*d*(D-H) / nm	*d*(H…A) / nm	*d*(D…A) / nm	∠DHA / (°)
O(4)–H(4)…N(2)A	0.082	0.185	0.267 1	174.3
O(5)–H(5)…O(9)B	0.082	0.182	0.262 0	163.6
O(10)–H(9)…O(6)C	0.082	0.185	0.265 5	166.9
O(11)–H(27)…N(4)D	0.082	0.185	0.266 5	177.8

Symmetry codes: A: $-x$, $-y+3$, $-z+1$; B: $x-1$, y, $z+1$; C: $x+1$, y, $z-1$; D: $-x+1$, $-y+1/2$, $-z+3$.

Table 4　Hydrogen bond parameters of compound 2

D–H…A	*d*(D-H) / nm	*d*(H…A) / nm	*d*(D…A) / nm	∠DHA / (°)
O(7)–H(1W)…O(5)A	0.082	0.193	0.275 1	174.8
O(7)–H(2W)…O(2)B	0.085	0.187	0.271 8	179.9
O(8)–H(4W)…O(10)C	0.085	0.174	0.258 6	179.8
O(9)–H(5W)…O(3)D	0.085	0.186	0.271 5	179.6
O(9)–H(6W)…O(6)	0.085	0.197	0.282 1	179.4
O(10)–H(7W)…O(4)E	0.085	0.205	0.290 2	179.5
O(10)–H(8W)…O(1)	0.085	0.186	0.270 9	179.4

Symmetry codes: A: x, y, $-z+1$; B: $-x+2$, $-y+1$, $-z+1$; C: $x+1$, y, z; D: $x-1$, y, z; E: $-x+2$, $-y+1$, $-z+2$.

2　Results and discussion

2.1　Description of the structure

2.1.1　$[Co(\mu_2\text{-}H_2btc)_2(4,4'\text{-bipy})_2]_n$ (**1**)

Single-crystal X-ray diffraction analysis reveals that compound **1** crystallizes in the triclinic space group $P\bar{1}$. The asymmetric unit of **1** contains one crystallographically unique Co(Ⅱ) ion, two μ_2-H_2btc^- blocks, and two 4,4′-bipy ligands. As shown in Fig.1, Co1 ion is six-coordinated by four O from four individual μ_2-H_2btc^- blocks and two N atoms from two different 4,4′-bipy ligands, constructing a distorted

octahedral geometry. The Co-O bond lengths range from 0.204 3(2) to 0.210 9(2) nm, whereas the Co-N bonds vary from 0.216 5(2) to 0.217 8(2) nm; these bonding parameters are comparable to those found in other reported Co(Ⅱ) compounds[13-15]. In **1**, the H_2btc^- ligand adopts the coordination mode Ⅰ (Scheme 1), in which a deprotonated carboxylate group shows a μ_2-η^1:η^1 bidentate mode. The dihedral angles of two benzene rings in the H_2btc^- ligands are 42.34° and 42.39°, respectively. The 4,4′-bpy ligands adopt a terminal coordination mode, their pyridyl rings are not coplanar showing the dihedral angles of 36.44° and 52.78°. The carboxylate groups of H_2btc^- blocks bridge alternately adjacent Co(Ⅱ) ions in a *syn-anti* coordination mode to form the infinite right-handed or left-handed helical Co-O-C-O-Co chains (Fig.2) with the Co⋯Co separation of 0.491 3(2) nm. Two types of these helical chains are interconnected to each other through the Co(Ⅱ) centers to produce double-helix chains. These chains are further extended into a 3D supramolecular framework via the O–H⋯O and O–H⋯N hydrogen-bonding interactions (Fig.3 and Table 3).

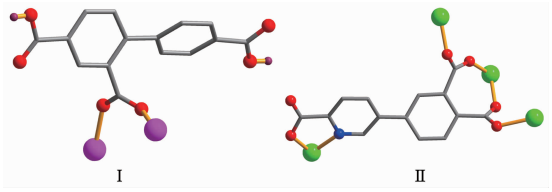

Scheme 1 Coordination modes of H_2btc^-/$dppa^{3-}$ ligands in compounds **1** and **2**

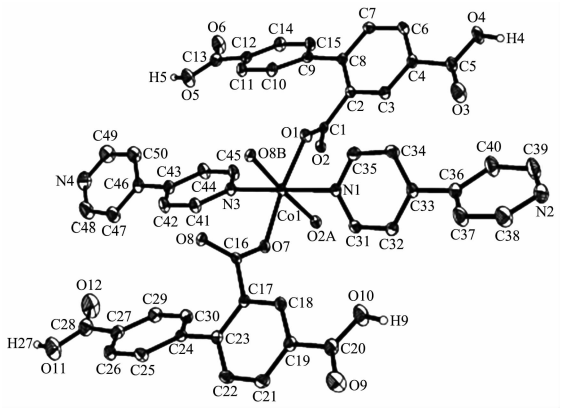

H atoms and lattice water molecules were omitted for clarity except H of COOH group; Symmetry codes: A: $-x$, $-y+2$, $-z+2$; B: $-x+1$, $-y+2$, $-z+2$

Fig.1 Drawing of the asymmetric unit of compound **1** with 30% probability thermal ellipsoids

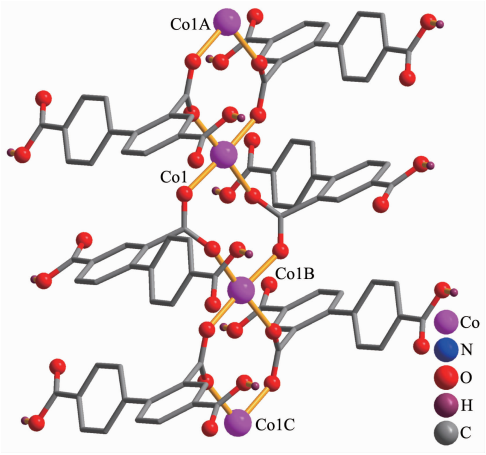

Symmetry codes: A: $-x+1$, $-y+2$, $-z+2$; B: $-x$, $-y+2$, $-z+2$; C: $x-1$, y, z

Fig.2 One dimesional double-helix chain in compound **1**

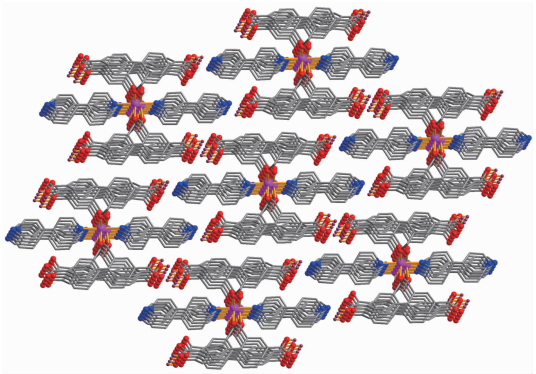

Fig.3 Perspective of 3D supramolecular framework along the *b* and *c* axes in **1**

2.1.2 $\{[Ni_3(\mu_4\text{-dppa})_2(H_2O)_6]\cdot 2H_2O\}_n$ (**2**)

The asymmetric unit of **2** possesses two crystallographically independent Ni(Ⅱ) ions (Ni1 having full occupancy, Ni2 having half occupancy), one $dppa^{3-}$ block, three H_2O ligands, and one lattice water molecule. As shown in Fig.4, the Ni1 atom is six-coordinated and adopts a distorted octahedral $\{NiNO_5\}$ geometry formed by three carboxylate O and one N atom from two distinct μ_4-$dppa^{3-}$ blocks and two O atoms from two water ligands. The six-coordinated Ni2 center is located on a 2-fold rotation axis and is surrounded by four O atoms from four different $dppa^{3-}$ blocks and two O atoms from two coordinated H_2O molecules, thus adopting a distorted octahedral $\{NiO_6\}$ geometry. The Ni-O distances range from 0.203 8(5) to 0.214 8(4) nm, whereas the Ni-N distance is 0.212 0(5) nm, and these bonding parameters agree

with those observed in other Ni(Ⅱ) compounds[13-14,16]. In **2**, the $dppa^{3-}$ block acts as a μ_4-spacer (mode Ⅱ, Scheme 1), in which the carboxylate groups exhibit the monodentate and the bidentate modes. In $dppa^{3-}$, the dihedral angle between the pyridyl and phenyl rings is 31.46°. Although 4,4′-bipy was added during the synthesis of **2**, a coordination of 4,4′-bipy to Ni(Ⅱ) is not observed in compound **2**. Interestingly, 4,4′-bipy acts as a template. The neighboring Ni(Ⅱ) ions are bridged by means of carboxylate groups from the $dppa^{3-}$ moieties, giving rise to a 1D chain (Fig.5). These 1D chains are multiply held together by the remaining COO^- groups and N atoms of the μ_4-$dppa^{3-}$ moieties to generate a 2D network (Fig.6).

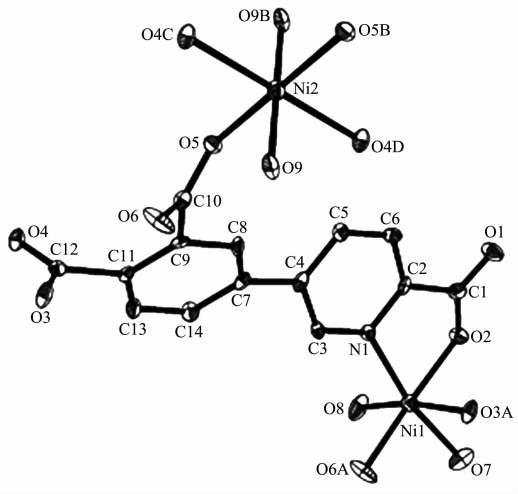

H atoms and lattice water molecules were omitted for clarity; Symmetry codes: A: $-x+2$, $-y+2$, $-z+2$; B: $-x+1$, $-y+2$, $-z+3$; C: $x-1$, y, z; D: $-x+2$, $-y+3$, $-z+3$

Fig.4　Drawing of the asymmetric unit of compound **2** with 30% probability thermal ellipsoids

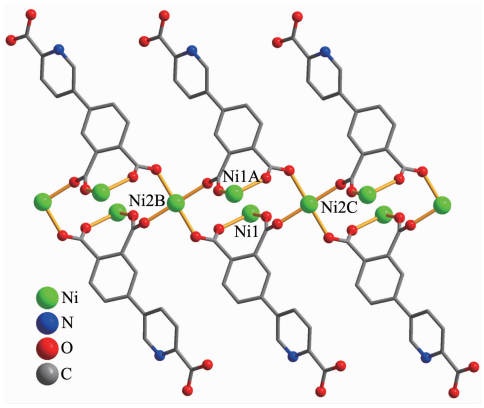

Symmetry codes: A: $-x+2$, $-y+2$, $-z+1$; B: x, y, $z-1$; C: $x+1$, y, $z-1$

Fig.5　One dimensional chain unit in compound **2**

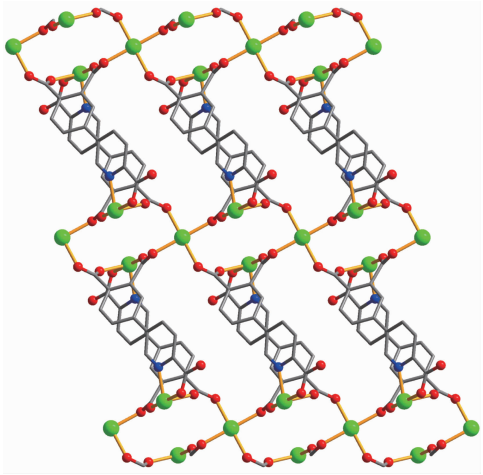

Fig.6　Perspective of a 2D network in **2** along the b and c axes

2.2　TGA analysis

To determine the thermal stability of polymers **1** and **2**, their thermal behaviors were investigated under nitrogen atmosphere by thermogravimetric analysis (TGA). As shown in Fig.7, TGA curve of compound **1** showed that the sample remained stable until 322 ℃, followed by a decomposition on further heating. Compound **2** lost its two lattice water molecules and six H_2O ligands in a range of 99 ~154 ℃ (Calcd. 16.2%, Obsd. 16.0%), followed by the decomposition at 281 ℃.

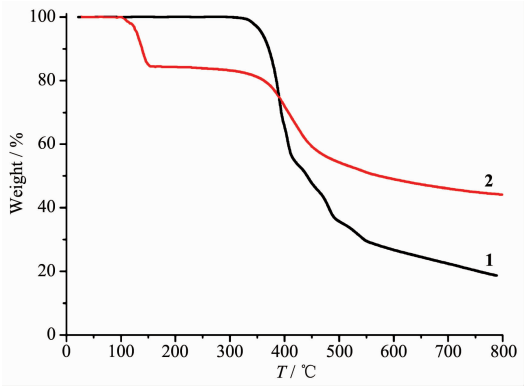

Fig.7　TGA curves of compounds **1** and **2**

2.3　Magnetic properties

Variable-temperature magnetic susceptibility measurements were performed on powder samples of **1** in the 2~300 K temperature range (Fig.8). As shown in Fig.8, the $\chi_M T$ value at room temperature was 3.83 $cm^3 \cdot mol^{-1} \cdot K$, which was higher than the value (1.87 $cm^3 \cdot mol^{-1} \cdot K$) for one magnetically isolated high-spin

Co(Ⅱ) ion (S=3/2, g=2.0). This is a common phenomenon for Co(Ⅱ) ions due to their strong spin-orbital coupling interactions[13-15]. Upon cooling, the value decreased gradually and reached a minimum of 3.23 $cm^3 \cdot mol^{-1} \cdot K$ at 17.4 K. Below 17.4 K, however, the $\chi_M T$ value increased rapidly to a maximum of 6.62 $cm^3 \cdot mol^{-1} \cdot K$ at 2.0 K. In the 30~300 K temperature range, the magnetic susceptibility obeyed the Curie-Weiss law, $\chi_M = C/(T-\theta)$, with θ=1.37 K, C=3.78 $cm^3 \cdot mol^{-1} \cdot K$. The positive θ value indicates the presence of dominant ferromagnetic interactions between the adjacent Co(Ⅱ) centers. According to the chain structure of **1** (Fig.2), there is one magnetic exchange pathway within the chain through two syn-anti carboxylate bridges, which could be responsible for the observed ferromagnetic exchange.

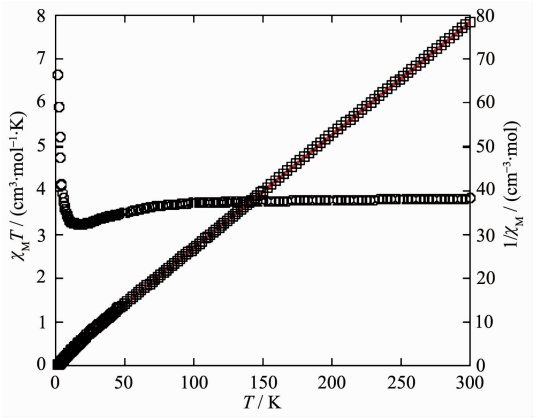

Red line shows the Curie-Weiss fitting

Fig.8 Temperature dependence of $\chi_M T$ (○) and $1/\chi_M$(□) vs T for compound **1**

3 Conclusions

In summary, we have successfully synthesized and characterized two new cobalt (**1**) and nickel (**2**) coordination polymers by using two biphenyl-type tricarboxylic acids as bridging ligands under hydrothermal conditions. The polymers **1** and **2** feature 1D double-helix chain and 2D network, respectively. Magnetic studies for compound **1** demonstrate a ferromagnetic coupling between the adjacent Co(Ⅱ) centers. The results show that such biphenyl-type tricarboxylic acids can be used as versatile multifunctional building blocks toward the generation of new coordination polymers. Moreover, 4,4′-bipyridine can tune the structures of the coordination polymers by its coordination or template effect.

References:

[1] Zheng X D, Lu T B. *CrystEngComm*, **2010**,**12**:324-336
[2] Yan W, Han L J, Jia, H L, et al. *Inorg. Chem.*, **2016**,**55**:8816-8821
[3] Li Q P, Du S W. *RSC Adv.*, **2015**,**5**:9898-9903
[4] Cui Y J, Yue Y F, Qian G D, et al. *Chem. Rev.*, **2012**,**12**:1126-1162
[5] Ou Y C, Gao X, Zhou Y, et al. *Cryst. Growth Des.*, **2016**,**16**:946-952
[6] Zeng M H, Yin Z, Tan Y X, et al. *J. Am. Chem. Soc.*, **2014**, **136**:4680-4688
[7] Gu J Z, Wen M, Cai Y, et al. *Inorg. Chem.*, **2019**,**58**:2403-2412
[8] Zou J Y, Li L, You S Y, et al. *Cryst. Growth Des.*, **2018**,**18**:3997-4003
[9] Zhang L N, Zhang C, Zhang B, et al. *CrystEngComm*, **2015**, **17**:2837-2846
[10]Du M, Li C P, Liu C S, et al. *Coord. Chem. Rev.*, **2013**,**257**:1282-1305
[11]Chen X M, Tong M L. *Acc. Chem. Res.*, **2007**,**40**:162-170
[12]Singh R, Bharatdwaj P K. *Cryst. Growth Des.*, **2013**,**13**:3722-3733
[13]Gu J Z, Gao Z Q, Tang Y. *Cryst. Growth Des.*, **2012**,**12**:3312-3323
[14]Gu J Z, Cui Y H, Liang X X, et al. *Cryst. Growth Des.*, **2016**,**16**:4658-4670
[15]GU Wen-Jun(顾文君), GU Jin-Zhong(顾金忠). *Chinese J. Inorg. Chem.*(无机化学学报), **2017**,**33**(2):227-236
[16]Gu J Z, Cai Y, Qian Z Y, et al. *Dalton Trans.*, **2018**,**47**:7431-7444
[17]Gu J Z, Cai Y, Wen M, et al. *Dalton Trans.*, **2018**,**47**:14327-14339
[18]Wu Y P, Wu X Q, Wang J F, et al. *Cryst. Growth Des.*, **2016**,**16**:2309-2316
[19]Liu B, Zhou H F, Guan Z H, et al. *Green Chem.*, **2016**,**18**:5418-5422
[20]ZHAO Su-Qin(赵素琴), GU Jin-Zhong(顾金忠). *Chinese J. Inorg. Chem.*(无机化学学报), **2016**,**32**(9):1611-1618
[21]Stock N, Biswas S. *Chem. Rev.*, **2012**,**112**:933-969
[22]Su J, Yao L D, Zhao M, et al. *Inorg. Chem.*, **2015**,**54**:6169-6175
[23]Chandrasekhar V, Mohapatra C, Butcher R J. *Cryst. Growth Des.*, **2012**,**12**:3285-3295
[24]Burd S D, Ma S, Perman J A, et al. *J. Am. Chem. Soc.*, **2012**,**134**:3663-3666
[25]Spek A L. *Acta Crystallogr. Sect. C: Struct. Chem.*, **2015**, **C71**:9-18